



Numerical solution of finite geometry boundary-value problems in nonlinear magnetoelasticity

R. Bustamante^{a,*}, A. Dorfmann^b, R.W. Ogden^{c,d}

^a Departamento de Ingeniería Mecánica, Universidad de Chile, Beaucheff 850, Santiago Centro, Santiago, Chile

^b Department of Civil and Environmental Engineering, Tufts University, Medford, MA 02155, USA

^c Department of Mathematics, University of Glasgow, Glasgow G12 8QW, UK

^d School of Engineering, University of Aberdeen, King's College, Aberdeen AB24 3UE, UK

ARTICLE INFO

Article history:

Received 16 September 2010

Received in revised form 22 November 2010

Available online 27 November 2010

Keywords:

Magnetoelasticity

Nonlinear elasticity

Finite deformation

Boundary-value problems

Numerical solution

ABSTRACT

This paper provides examples of the numerical solution of boundary-value problems in nonlinear magnetoelasticity involving finite geometry based on the theoretical framework developed by Dorfmann and co-workers. Specifically, using a prototype constitutive model for isotropic magnetoelasticity, we consider two two-dimensional problems for a block with rectangular cross-section and of infinite extent in the third direction. In the first problem the deformation induced in the block by the application of a uniform magnetic field far from the block and normal to its larger faces without mechanical load is examined, while in the second problem the same magnetic field is applied in conjunction with a shearing deformation produced by in-plane shear stresses on its larger faces. For each problem the distribution of the magnetic field throughout the block and the surrounding space is illustrated graphically, along with the corresponding deformation of the block. The rapidly (in space) changing magnitude of the magnetic field in the neighbourhood of the faces of the block is highlighted.

© 2010 Elsevier Ltd. All rights reserved.

1. Introduction

Considerable interest has developed in recent years in polymer-based mechanically soft materials possessing high magneto-mechanical compliance, and they are capable of large elastic deformations under the influence of an external magnetic field, much larger than in conventional magnetostriction (Bednarek, 1999; Ginder et al., 2002). Typical of these newly synthesized materials are highly deformable and magnetizable elastomers, which are composed of a rubber-like matrix embedded with micron-sized magneto-active particles (Jolly et al., 1996; Lokander and Stenberg, 2003; Boczkowska and Awietjan, 2009).

The magneto-mechanical response of these materials is highly nonlinear and the magneto-mechanical coupling offers the possibility of developing new devices for a variety of applications, including, actuators, sensors, dampers and control systems; see, for example, Ginder et al. (1999, 2000, 2001), Albanese and Cune-fare (2003), Farshad and Le Roux (2004), Yalcintas and Dai (2004), and the review by Li and Zhang (2008). Some relevant experimental data can be found in Bellan and Bossis (2002), Bossis et al. (2001), Varga et al. (2005, 2006), for example. Of crucial importance is the nonlinearity, and the advent of materials that can oper-

ate in a highly nonlinear magneto-mechanical regime presents challenges from both practical and theoretical perspectives.

At present the influence of magnetic fields on the behaviour of magneto-sensitive materials in the highly nonlinear regime is not well understood and the development of an appropriate theoretical framework is essential to further that understanding. These new materials have stimulated the constitutive modelling for the description of their magneto-mechanical properties, and a theoretical framework for the analysis of these materials has been developed; see, in particular, Brigadnov and Dorfmann (2003), Dorfmann and Ogden (2003, 2004a,b, 2005a,b), Bustamante (2010), and related developments by Kankanala and Triantafyllidis (2004) and Steigmann (2004). For the relevant background on magnetoelasticity and electromagnetic–mechanical interactions in general, see Brown (1966), Maugin (1988), Eringen and Maugin (1990), Kovetz (2000), Hutter et al. (2006), and the collection of lecture notes in the volume edited by Ogden and Steigmann (in press).

In this paper we are concerned with the solution of basic boundary-value problems in nonlinear magnetoelasticity. There are very few exact (closed-form) solutions available, and those that are available relate to idealized geometries of infinite extent, such as a slab of material of uniform finite thickness extending to infinity in two directions or an infinitely long circular cylindrical tube. For finite geometries, in contrast to the situation in pure nonlinear elasticity theory, there is a need to obtain solutions that satisfy the

* Corresponding author.

E-mail address: rogbusta@ing.uchile.cl (R. Bustamante).

magnetic boundary conditions on all interfaces between the material and the surrounding space, and this is the source of the difficulty of obtaining solutions analytically. Accordingly, to obtain solutions it is necessary in general to adopt a numerical approach.

In Section 2 we summarize briefly the relevant kinematics of finite deformation, the equations of magnetoelastostatics, and then, based on the formulation of nonlinear magnetoelasticity in Dorfmann and Ogden (2004b, 2005a,b), the equations of mechanical equilibrium, the associated boundary conditions, the constitutive law of a magnetoelastic material, and its isotropic specialization based on the theory of invariants. The formulation of a general boundary-value problem of magnetoelasticity is presented in Section 3 and a prototype constitutive law is adopted as the basis for the numerical solutions in Section 4. In a previous paper (Bustamante et al., 2007) we used a finite difference method to obtain the distribution of the magnetic field within and exterior to a hollow circular cylinder of finite length that was subjected to uniform extension and radial inflation (or deflation) but held in a circular cylindrical configuration. In the present paper no such assumption on the deformation is made and the material is free to deform under the influence of an applied magnetic field, subject in one example also to applied mechanical loads.

In Section 4 we obtain numerical (finite element) solutions for two problems involving a rectangular block of finite uniform cross-section, based on use of the multiphysics package (Comsol Multiphysics, 2007). In the first problem the deformation induced in the block by the application of a uniform magnetic field far from the block and normal to its larger faces without mechanical load is examined, while in the second problem the same magnetic field is applied in conjunction with a shearing deformation produced by in-plane shear stress on its larger faces. For each problem the distribution of the magnetic field throughout the block and the surrounding space is illustrated graphically, along with the corresponding deformation of the block. The sharply varying magnitude of the magnetic field in the neighbourhood of the faces of the block is highlighted.

Some concluding remarks are contained in Section 5.

2. Basic equations

2.1. Kinematics

Consider a deformable magnetoelastic body that is initially in an unstressed configuration, denoted \mathcal{B}_0 , with boundary $\partial\mathcal{B}_0$, within three-dimensional Euclidean space. Let the position vector \mathbf{X} of a point in \mathcal{B}_0 identify the material particle located at that point. Under the action of applied mechanical loads combined with an applied magnetic field the body deforms quasi-statically into a new (deformed) configuration, denoted \mathcal{B} , with boundary $\partial\mathcal{B}$. Suppose the material particle \mathbf{X} occupies the new position $\mathbf{x} = \boldsymbol{\chi}(\mathbf{X})$ in \mathcal{B} , where the vector field $\boldsymbol{\chi}$ describes the deformation of the body, is defined for $\mathbf{X} \in \mathcal{B}_0 \cup \partial\mathcal{B}_0$ and is endowed with suitable regularity properties.

The deformation gradient tensor \mathbf{F} relative to \mathcal{B}_0 is defined by $\mathbf{F} = \text{Grad}\boldsymbol{\chi}$, where Grad denotes the gradient operator with respect to \mathbf{X} . We also use the notation $J = \det\mathbf{F}$, noting that, by convention, $J > 0$. The right and left Cauchy–Green tensors associated with \mathbf{F} are defined by

$$\mathbf{c} = \mathbf{F}^T\mathbf{F}, \quad \mathbf{b} = \mathbf{F}\mathbf{F}^T, \quad (1)$$

respectively, where T indicates the transpose (of a second-order tensor). We remark that in the continuum mechanics literature the left Cauchy–Green tensor is normally denoted \mathbf{B} , which conflicts with the standard notation for the magnetic induction vector. To avoid this conflict lower case characters \mathbf{c} and \mathbf{b} are used here for the Cauchy–Green tensors.

In order to distinguish differential operators, such as grad, div and curl, with respect to \mathbf{x} from those with respect to \mathbf{X} , the notations Grad, Div and Curl are used in the latter case. We also adopt the convention that when applied to tensors the divergence operators act on the left leg of the tensor that follows them. For example, for any uniform vector \mathbf{a} in \mathcal{B} , $\text{Div}(\mathbf{F}^T)$ is defined by $\text{Div}(\mathbf{F}^T) \cdot \mathbf{a} \equiv \text{Div}(\mathbf{F}^T\mathbf{a})$. For background on the relevant nonlinear elasticity theory, see, for example, Ogden (1997, 2001).

2.2. Magnetostatics

Let \mathbf{B} denote the magnetic induction vector and \mathbf{H} the magnetic field vector in configuration \mathcal{B} . In free space (or non-magnetizable material) they are related by

$$\mathbf{B} = \mu_0\mathbf{H}, \quad (2)$$

where the constant μ_0 is the permeability of free space. In magnetizable material (2) does not hold, and an additional vector field, the magnetization \mathbf{M} , is defined by the difference

$$\mathbf{M} = \mu_0^{-1}\mathbf{B} - \mathbf{H}. \quad (3)$$

This characterizes the response of the material to an external magnetic field, but must be accompanied by a constitutive law that describes the magnetic properties of the considered material. Such a law gives one of the three magnetic vectors above in terms of one of the others, and there are several options for specifying such a relationship.

In the present paper we consider only time-independent deformations and magnetic fields and we assume that there are no free currents within the material. Then, \mathbf{B} and \mathbf{H} satisfy the following specializations of Maxwell’s equations

$$\text{div}\mathbf{B} = 0, \quad \text{curl}\mathbf{H} = \mathbf{0}. \quad (4)$$

These apply both within and outside the material. For detailed background on electromagnetic theory, see, for example, the classic text by Jackson (1999).

In the absence of free surface currents the continuity conditions

$$\mathbf{n} \cdot \llbracket \mathbf{B} \rrbracket = 0, \quad \mathbf{n} \times \llbracket \mathbf{H} \rrbracket = \mathbf{0}, \quad (5)$$

are satisfied on the boundary $\partial\mathcal{B}$, where $\llbracket \bullet \rrbracket$ signifies a discontinuity across the boundary $\partial\mathcal{B}$ and \mathbf{n} is the outward unit normal to $\partial\mathcal{B}$. For example, $\llbracket \mathbf{B} \rrbracket = \mathbf{B}^\circ - \mathbf{B}^i$, where $^\circ$ and i signify “outside” and “inside” the material, respectively. Using Eqs. 2 and 3, valid respectively outside and inside the material, the boundary conditions (5) can be written equivalently as

$$\llbracket \mathbf{B} \rrbracket = \mu_0\mathbf{n} \times (\mathbf{n} \times \mathbf{M}), \quad \llbracket \mathbf{H} \rrbracket = (\mathbf{n} \cdot \mathbf{M})\mathbf{n}. \quad (6)$$

Equations (4) are Eulerian in form and involve the operators div and curl. We now introduce the Lagrangian counterparts of \mathbf{B} and \mathbf{H} , denoted \mathbf{B}_l and \mathbf{H}_l and defined by

$$\mathbf{B}_l = J\mathbf{F}^{-1}\mathbf{B}, \quad \mathbf{H}_l = \mathbf{F}^T\mathbf{H}. \quad (7)$$

Then the kinematical identities

$$J\text{div}\mathbf{B} = \text{Div}(J\mathbf{F}^{-1}\mathbf{B}), \quad J\mathbf{F}^{-1}\text{curl}\mathbf{H} = \text{Curl}(\mathbf{F}^T\mathbf{H}), \quad (8)$$

enable Eqs. (4) to be recast in the Lagrangian forms

$$\text{Div}\mathbf{B}_l = 0, \quad \text{Curl}\mathbf{H}_l = \mathbf{0}. \quad (9)$$

The corresponding Lagrangian forms of the boundary conditions are

$$\mathbf{N} \cdot \llbracket \mathbf{B}_l \rrbracket = 0, \quad \mathbf{N} \times \llbracket \mathbf{H}_l \rrbracket = \mathbf{0}, \quad (10)$$

where \mathbf{N} is the unit outward normal to the reference boundary $\partial\mathcal{B}_0$ associated with \mathbf{n} through Nanson’s formula $\mathbf{n}d\mathbf{a} = J\mathbf{F}^{-T}\mathbf{N}d\mathbf{A}$, where $d\mathbf{A}$ and $d\mathbf{a}$ are area elements on $\partial\mathcal{B}_0$ and $\partial\mathcal{B}$, respectively.

2.3. Magneto-mechanical equilibrium

In what follows we assume that there are no mechanical body forces. Magnetic body forces can be treated equivalently as stresses by introducing the so-called *total* (Cauchy) stress tensor $\boldsymbol{\tau}$, which is a symmetric tensor (see, for example, Dorfmann and Ogden, 2004b). The equilibrium equation can then be written simply as

$$\operatorname{div} \boldsymbol{\tau} = \mathbf{0}, \quad (11)$$

where $\boldsymbol{\tau}$ satisfies the boundary condition

$$\boldsymbol{\tau} \mathbf{n} = \mathbf{t}_a + \mathbf{t}_m \quad \text{on } \partial \mathcal{B}. \quad (12)$$

In (12) \mathbf{t}_a is the mechanical traction (per unit area) applied on $\partial \mathcal{B}$ and $\mathbf{t}_m = \boldsymbol{\tau}_m \mathbf{n}$, where $\boldsymbol{\tau}_m$ is the Maxwell stress evaluated on the outside of $\partial \mathcal{B}$. The Maxwell stress is defined by

$$\boldsymbol{\tau}_m = \mathbf{B} \otimes \mathbf{H} - \frac{1}{2} \mu_0 (\mathbf{H} \cdot \mathbf{H}) \mathbf{I}, \quad (13)$$

where \mathbf{I} is the identity. Here the Maxwell stress is used only outside the material, where (2) holds and $\operatorname{div} \boldsymbol{\tau}_m = \mathbf{0}$.

2.4. Constitutive equations

In order to solve boundary-value problems we require constitutive equations that give the total stress $\boldsymbol{\tau}$ and a magnetic vector in terms of the deformation gradient \mathbf{F} and an independent magnetic variable. Here, we choose to use \mathbf{H} as the independent magnetic vector and to give \mathbf{B} by a constitutive law. Since $\operatorname{curl} \mathbf{H} = \mathbf{0}$, this involves working with a scalar potential $\varphi = \varphi(\mathbf{x})$ such that $\mathbf{H} = -\operatorname{grad} \varphi$. The remaining equations, $\operatorname{div} \mathbf{B} = \mathbf{0}$ and $\operatorname{div} \boldsymbol{\tau} = \mathbf{0}$, must then be solved for $\mathbf{x} = \boldsymbol{\chi}(\mathbf{X})$ and $\varphi(\mathbf{x})$.

There are many different ways in which constitutive equations for magnetoelastic materials can be constructed, and for a recent overview of several possible formulations we refer to Bustamante et al. (2008). In Dorfmann and Ogden (2004b), for example, a theory of magnetoelasticity using \mathbf{F} and \mathbf{B}_l as the independent variables was developed in terms of an energy (or potential) function $\Omega = \Omega(\mathbf{F}, \mathbf{B}_l)$, defined per unit reference volume. In the same paper an alternative formulation involving an energy function $\Omega_*(\mathbf{F}, \mathbf{H}_l)$ was also noted, and it is this latter function that we use here. In terms of this (total) energy function the (total) nominal stress tensor $\mathbf{T} \equiv \mathbf{J} \mathbf{F}^{-1} \boldsymbol{\tau}$ and the Lagrangian magnetic induction vector \mathbf{B}_l are obtained simply as

$$\mathbf{T} = \frac{\partial \Omega^*}{\partial \mathbf{F}}, \quad \mathbf{B}_l = -\frac{\partial \Omega^*}{\partial \mathbf{H}_l}. \quad (14)$$

The corresponding Eulerian quantities are

$$\boldsymbol{\tau} = \mathbf{J}^{-1} \mathbf{F} \frac{\partial \Omega^*}{\partial \mathbf{F}}, \quad \mathbf{B} = -\mathbf{J}^{-1} \mathbf{F} \frac{\partial \Omega^*}{\partial \mathbf{H}_l}. \quad (15)$$

2.4.1. Isotropic magnetoelastic solids

From this point on we specialize the constitutive equations to those appropriate for *isotropic* magnetoelastic materials. For such materials the constitutive equations can be expressed in terms of six independent invariants involving the deformation, via the right Cauchy–Green tensor \mathbf{c} , and the (Lagrangian) magnetic field vector \mathbf{H}_l . The magnetoelastic material is said to be *isotropic* if Ω_* is an isotropic function of \mathbf{c} and $\mathbf{H}_l \otimes \mathbf{H}_l$. Note that the latter expression is unaffected by reversal of the sign of \mathbf{H}_l . Then, the form of Ω_* is reduced to dependence on the principal invariants I_1, I_2, I_3 of \mathbf{c} , defined by

$$I_1 = \operatorname{tr} \mathbf{c}, \quad I_2 = \frac{1}{2} \left[(\operatorname{tr} \mathbf{c})^2 - \operatorname{tr}(\mathbf{c}^2) \right], \quad I_3 = \det \mathbf{c} = \mathbf{J}^2, \quad (16)$$

together with three invariants that depend on \mathbf{H}_l . These are denoted here by I_4, I_5, I_6 and possible choices for their definitions, which we use here, are

$$I_4 = |\mathbf{H}_l|^2, \quad I_5 = (\mathbf{c} \mathbf{H}_l) \cdot \mathbf{H}_l, \quad I_6 = (\mathbf{c}^2 \mathbf{H}_l) \cdot \mathbf{H}_l. \quad (17)$$

For a general reference to the theory of invariants of tensors and vectors we cite Spencer (1971).

A direct calculation based on (15)₁ leads to

$$\boldsymbol{\tau} = \mathbf{J}^{-1} \left[2\Omega_1^* \mathbf{b} + 2\Omega_2^* (I_1 \mathbf{b} - \mathbf{b}^2) + 2I_3 \Omega_3^* \mathbf{I} + 2\Omega_5^* \mathbf{b} \mathbf{H} \otimes \mathbf{b} \mathbf{H} + 2\Omega_6^* (\mathbf{b} \mathbf{H} \otimes \mathbf{b}^2 \mathbf{H} + \mathbf{b}^2 \mathbf{H} \otimes \mathbf{b} \mathbf{H}) \right], \quad (18)$$

which is clearly symmetric, and we recall that $\mathbf{b} = \mathbf{F} \mathbf{F}^T$ is the left Cauchy–Green deformation tensor. The corresponding expression for \mathbf{B} is obtained from (15)₂ as

$$\mathbf{B} = -2\mathbf{J}^{-1} \left(\Omega_4^* \mathbf{b} \mathbf{H} + \Omega_5^* \mathbf{b}^2 \mathbf{H} + \Omega_6^* \mathbf{b}^3 \mathbf{H} \right). \quad (19)$$

In the above equations Ω_i^* is defined as $\partial \Omega^* / \partial I_i$ for $i = 1, \dots, 6$. The corresponding Lagrangian forms may be obtained from the connections $\mathbf{T} = \mathbf{J} \mathbf{F}^{-1} \boldsymbol{\tau}$ and $\mathbf{B}_l = \mathbf{J} \mathbf{F}^{-1} \mathbf{B}$. However, in what follows we work in terms of the Eulerian form of the governing equations. A generalization of the above isotropic model to the transversely isotropic case has been developed by Bustamante (2010).

3. Boundary-value problem formulation

Here we outline briefly a general approach towards obtaining solutions of boundary-value problems in nonlinear magnetoelasticity, and we restrict attention to situations in which there is no mechanical body force. Then, the relevant equations to be solved are (in Eulerian form)

$$\operatorname{div} \mathbf{B} = \mathbf{0}, \quad \operatorname{curl} \mathbf{H} = \mathbf{0}, \quad \operatorname{div} \boldsymbol{\tau} = \mathbf{0}, \quad (20)$$

together with the jump conditions (5) at a material interface (which here is just the boundary $\partial \mathcal{B}$) and the constitutive Eqs. (18) and (19).

Equation (20)₂ enables us to use the magnetic scalar potential $\varphi = \varphi(\mathbf{x})$, so that

$$\mathbf{H} = -\operatorname{grad} \varphi. \quad (21)$$

Equation (21) is valid inside the material and the surrounding space. In the surrounding space we have $\operatorname{div} \mathbf{H} = 0$ and the magnetic potential φ must satisfy Laplace's equation

$$\nabla^2 \varphi = 0. \quad (22)$$

Inside the material, on the other hand, we have $\operatorname{div} \mathbf{B} = 0$, where \mathbf{B} is the function of \mathbf{F} and \mathbf{H} given by (19). For convenience and using (21), we rewrite the constitutive equation in compact form as

$$\mathbf{B} = -\mathcal{C}^* \mathbf{H} = \mathcal{C}^* \operatorname{grad} \varphi, \quad (23)$$

where \mathcal{C}^* is defined by

$$\mathcal{C}^* = 2\mathbf{J}^{-1} \left(\Omega_4^* \mathbf{b} + \Omega_5^* \mathbf{b}^2 + \Omega_6^* \mathbf{b}^3 \right), \quad (24)$$

and we emphasize that in general Ω_4^*, Ω_5^* and Ω_6^* depend on \mathbf{F} and \mathbf{H} through the invariants (16) and (17), with $\mathbf{H}_l = \mathbf{F}^T \mathbf{H}$. Inside the material, instead of (22), the magnetic potential φ has to satisfy

$$\operatorname{div}(\mathcal{C}^* \operatorname{grad} \varphi) = 0. \quad (25)$$

Therefore, the general boundary-value problem aims to determine $\varphi(\boldsymbol{\chi}(\mathbf{X}))$ and $\boldsymbol{\chi}(\mathbf{X})$ for a given reference geometry \mathcal{B}_0 and requires solution of Eq. (22) in the surrounding space and Eqs. (25) and (20)₃ with (18) within \mathcal{B}_0 , the solutions being connected by the continuity conditions (5).

3.1. Volumetric–dilatational decomposition for compressible materials

In the numerical solution of boundary-value problems involving compressible materials, which we consider in Section 4, it will be convenient to adopt a decomposition of the deformation gradient into volume preserving and dilatational contributions. Following Flory (1961) and Ogden (1976, 1978), we consider the decomposition

$$\mathbf{F} = (J^{1/3}\mathbf{I})\bar{\mathbf{F}}, \quad (26)$$

where the modified deformation gradient $\bar{\mathbf{F}}$ describes the volume-preserving part of the deformation, while the dilatational part is given in terms of $J = \det \mathbf{F}$. It follows from (26) that $\det \bar{\mathbf{F}} = 1$. The associated modified right and left Cauchy–Green tensors are given respectively by

$$\bar{\mathbf{c}} = \bar{\mathbf{F}}^T \bar{\mathbf{F}} = J^{-2/3} \mathbf{c}, \quad \bar{\mathbf{b}} = \bar{\mathbf{F}} \bar{\mathbf{F}}^T = J^{-2/3} \mathbf{b}, \quad (27)$$

and we recall the Cauchy–Green tensors defined in (1).

The invariants defined in (16) and (17) are modified accordingly when the modified Cauchy–Green tensors are used in the formulation of constitutive equations. The modified invariants are given by

$$\bar{I}_1 = J^{-2/3} I_1, \quad \bar{I}_2 = J^{-4/3} I_2, \quad \bar{I}_3 \equiv 1, \quad (28)$$

and

$$\bar{I}_4 = I_4, \quad \bar{I}_5 = J^{-2/3} I_5, \quad \bar{I}_6 = J^{-4/3} I_6. \quad (29)$$

3.2. A prototype energy function

As a basis for numerical calculations particular forms of the energy function Ω^* are needed, and in order to predict realistic behaviour in representative boundary-value problems such energy functions should be compatible with data from (magneto-mechanical) experimental tests on the materials in question. Unfortunately, the data available on magneto-sensitive elastomers of the kind required are limited, although some relevant data can be found in the papers by Ginder et al. (1999), Bossis et al. (2001), Bellan and Bossis (2002), and Varga et al. (2005, 2006), for example. Data therein were used by Bustamante (2010) to construct a form of the energy function Ω^* for transversely isotropic magneto-sensitive elastomers. Here we use an isotropic specialization of the model having the decoupled representation

$$\Omega^* = \Omega_{\text{iso}}^* + \Omega_{\text{vol}}^* + \Omega_0^*, \quad (30)$$

where Ω_{iso}^* and Ω_{vol}^* are, respectively, isochoric and volumetric contributions given by

$$\begin{aligned} \Omega_{\text{iso}}^* = & \frac{1}{2}(g_0 + g_1 I_4)(\bar{I}_1 - 3) - m_0 m_1 \log \left[\cosh \left(\frac{\sqrt{I_4}}{m_1} \right) \right] - c_0 I_4 \\ & + c_1 \mu_0 \bar{I}_5, \end{aligned} \quad (31)$$

and

$$\Omega_{\text{vol}}^* = \frac{1}{2} \kappa (J - 1)^2, \quad (32)$$

Ω_0^* is a constant that is included to ensure that Ω^* vanishes in the reference configuration \mathcal{B}_0 , and $g_0, g_1, m_0, m_1, c_0 = \mu_0(c_1 - 1)/2$ and κ , together with the free-space permeability μ_0 , are constants. For the numerical calculations in Section 4 these parameters have values given in Table 1.

Based on (30), with Ω^* now treated as a function of $\bar{I}_1, \bar{I}_4, \bar{I}_5$ and J , the expressions for the total stress (18) and magnetic induction (19) in the material become

Table 1
Values of the material parameters in (31) and (32).

g_0 (Pa)	g_1 (PaA ⁻² m ²)	m_0 (T)	m_1 (Am ⁻¹)	c_1	μ_0 (NA ⁻²)	κ (Pa)
10 ⁵	-10 ⁻⁶	0.4998	309339.5	1250	1.2566 · 10 ⁻⁶	10 ⁵

$$\boldsymbol{\tau} = 2J^{-1} \left[\bar{\Omega}_1^* \left(\bar{\mathbf{b}} - \frac{1}{3} \bar{I}_1 \mathbf{1} \right) + \bar{\Omega}_2^* J^{2/3} \left(\bar{\mathbf{b}} \mathbf{H} \otimes \bar{\mathbf{b}} \mathbf{H} - \frac{1}{3} \mathbf{H} \cdot (\bar{\mathbf{b}}^2 \mathbf{H}) \mathbf{1} \right) \right] + \bar{\Omega}_j^* \mathbf{1}, \quad (33)$$

and

$$\mathbf{B} = -2J^{-1/3} \left(\bar{\Omega}_4^* \bar{\mathbf{b}} \mathbf{H} + \bar{\Omega}_5^* \bar{\mathbf{b}}^2 \mathbf{H} \right), \quad (34)$$

where $\bar{\Omega}_i^* = \partial \Omega^* / \partial \bar{I}_i, i = 1, 4, 5$, and $\bar{\Omega}_j^* = \partial \Omega^* / \partial J$. We recall that $\bar{\mathbf{b}}$ is the modified left Cauchy–Green tensor defined by (27)₂ and that \mathbf{H} is the magnetic field given in terms of the scalar potential by $\mathbf{H} = -\text{grad } \varphi$. Outside the material $\mathbf{B} = \mu_0 \mathbf{H}$ and φ satisfies the Eq. (22), while inside the material it satisfies Eq. (25).

4. Application to a rectangular block

In a previous paper (Dorfmann and Ogden, 2005b) we considered the deformation of a slab of magnetoelastic material of finite thickness and parallel plane faces of infinite extent. The slab was subject to a uniform magnetic field normal to its faces and solutions corresponding to two separate homogeneous deformations were obtained: pure homogeneous deformation and simple shear. It is important to note that the infinite lateral extent of the slab enabled exact solutions to be obtained because the magnetic boundary conditions could be satisfied exactly. Such exact (closed-form) solutions are not in general possible when the material body has finite dimensions since in such situations the continuity conditions for \mathbf{B} and \mathbf{H} on the finite boundaries cannot be satisfied for solutions given in terms of simple functions and it is therefore necessary to adopt a numerical approach to the solution of the boundary-value problems in question.

In the present paper we consider a block of material of rectangular cross-section and infinite extent in the direction normal to the cross-section as a (two-dimensional, plane strain) vehicle for developing numerical solutions that enable the distributions of the magnetic field and the magnetic induction to be determined both within the material and in the surrounding space.

Consider then a block of magnetoelastic material infinite in extent in the X_3 direction and with rectangular cross-section (independent of X_3) of finite dimensions in the (X_1, X_2) plane in the reference configuration. The deformation to be considered is one of plane strain in the (X_1, X_2) plane and the magnetic field is taken to lie within the plane and to be independent of X_3 so as to restrict attention to a two-dimensional problem. For numerical purposes the dimensions (length and thickness) of the rectangular cross-section of the block in the X_1 and X_2 directions are set as $L_b = 0.2$ m and $T_b = 0.04$ m, respectively, resulting in an aspect ratio of 5, while it suffices to take the corresponding dimensions of the surrounding free space as $L_f = 4$ m and $T_f = 2$ m, giving an aspect ratio of 2. The dimensions of the exterior region have been chosen to ensure that the magnetic field at its outer extremities is essentially uniform, and that this is the case is confirmed by the example considered in Section 4.1 below (as reflected in Figs. 3–5). The considered rectangular region and the surrounding space for which the governing equations and boundary conditions are to be solved are depicted in Fig. 1, but, for clarity, not shown to scale.

Fig. 2 shows a detailed quarter view of the layout of the finite element mesh within the magnetoelastic material and in part of the surrounding space; continuity conditions need to be satisfied

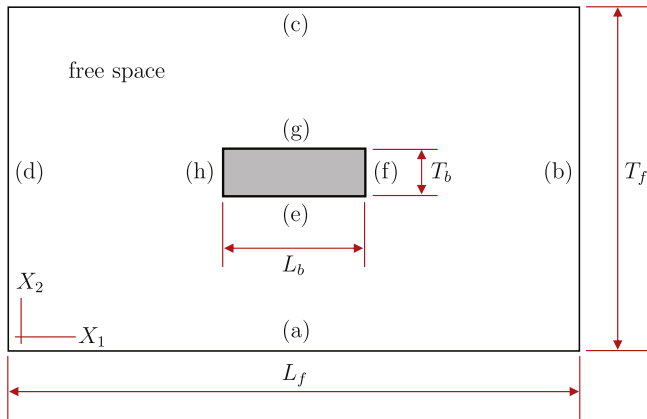


Fig. 1. Geometric layout of the rectangular cross-section of the magnetoelastic body and the surrounding space. The space surrounding the material is defined by $-2 \leq X_1 \leq 2$, $-1 \leq X_2 \leq 1$, and the material is located in the region $-0.1 \leq X_1 \leq 0.1$, $-0.02 \leq X_2 \leq 0.02$, the dimensions being metres (not drawn to scale).

by \mathbf{B} and \mathbf{H} across the interface, which is indicated by the solid line. The finite elements are triangular, of Lagrange quadratic type (each element has 6 nodes): in the material, 6860 elements are used, and in the surrounding space, 27176 elements, with 95927 degrees of freedom.

The first example does not involve any mechanical body forces or surface tractions, and the deformation produced in the material is entirely due to the application of a magnetic field. The second example considers the material subject to shear deformation generated by the application of a mechanical traction in the presence of a magnetic field.

Because the problem is two dimensional the scalar potential φ depends only on the coordinates x_1 , x_2 in the deformed configuration. For each of the examples the applied magnetic field is the same and corresponds to a uniform magnetic field applied 'at infinity' in the X_2 direction. This is approximated for the finite region of the (two-dimensional) space surrounding the material by taking the component H_1 of the magnetic field to vanish on the exterior boundaries (a) and (c) shown in Fig. 1. This effectively means the far-field magnetic boundary condition is that the scalar potential φ has a constant value on each of (a) and (c), say φ_a and φ_c , respectively. On each of the other exterior boundaries (b) and (d) we may take the boundary condition as $H_1 = 0$ and then there is a uniform field component $H_2 = H$ parallel to the boundary, and on (b) and (d) we therefore have $\varphi = -HX_2 + c$, where c is a constant. For compatibility we must have $c = (\varphi_a + \varphi_c)/2$ and $\varphi_a - \varphi_c = HT_f$.

Due to the interaction with the body, the magnetic field lines deviate near the material boundaries so as to satisfy the continuity conditions (5) and must therefore depend on both coordinates x_1 and x_2 . We may take φ to be continuous across the boundary between the material and the surrounding space. This then guarantees that the tangential component of \mathbf{H} is continuous across the boundary, as required by the boundary condition (5)₂. Thus, referring to Fig. 1, H_1 is continuous across the boundaries (e) and (g) and H_2 is continuous across (f) and (h). It remains to consider the boundary condition (5)₁, i.e. $\mathbf{n} \cdot [\mathbf{B}] = 0$. This requires that the component B_2 be continuous across the boundaries (e) and (g), and that B_1 be continuous across (f) and (h). To reduce possible numerical problems associated with singularities at the corners, in the numerical calculations the corners have been taken as slightly rounded with radius 1 mm.

Solutions of Eqs. (22) and (25) are needed to determine the magnetic field and stress distributions. To obtain these numerically we select, as the starting point, the *linear electroelastic* option implemented in a multiphysics code (Comsol Multiphysics, 2007). This code allows modelling of a piezoelectric body surrounded by free space. We modified the electrostatic equations implemented in Comsol to account for large deformation kinematics and nonlinear *magnetoelasticity* and used these to solve the governing Eq. (20) inside the material and in the surrounding free space, satisfying the required jump conditions on the material surfaces. For the free space the Comsol tool 'Moving Mesh (ALE)' was used to deform the exterior mesh to accommodate the deformation of the material (this was originally developed for fluid–structure interaction problems; see Comsol Multiphysics User Guide, Structural Mechanics Module, pp. 356–360). For solving the system of nonlinear algebraic equations the 'Damped Newton Method' was used with relative tolerance 10^{-6} and maximum number of iterations 120, and for highly nonlinear problems an initial damping factor of 10^{-4} and minimum damping factor 10^{-16} (see Comsol Multiphysics Reference Guide, Version 3.5a, Chapter 5, pp. 533–536). Linearization of the equations is automatically taken care of within Comsol, although it is not clear from the documentation whether this is done before or after the finite element implementation.

4.1. Example 1: magnetic field induced deformation

In this example no mechanical loads are applied to the body and the deformation induced in the material is due entirely to the applied magnetic field. To restrain the body from any rigid translation the material point located at the center of the edge (e) is not allowed to displace in the X_1 direction, and to eliminate rigid body

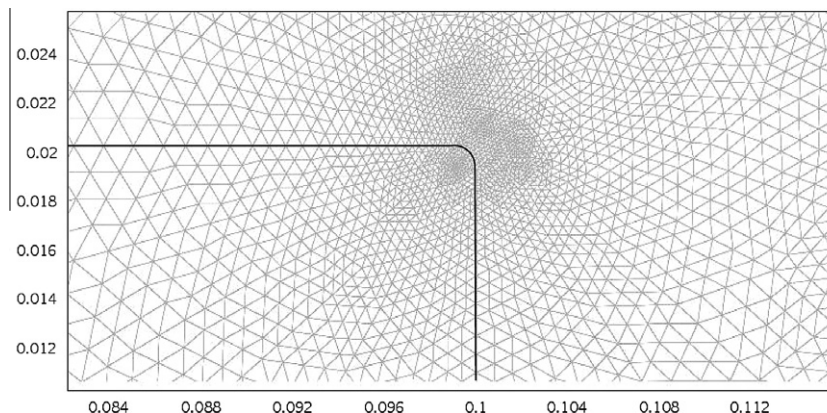


Fig. 2. Detailed view of the (triangular) element size distribution in the upper right corner of the material and in the surrounding space. The element size depends on the spatial gradient of the magnetic vector fields, the elements being smallest in regions where the largest variations in the magnetic field and magnetic induction vectors occur.

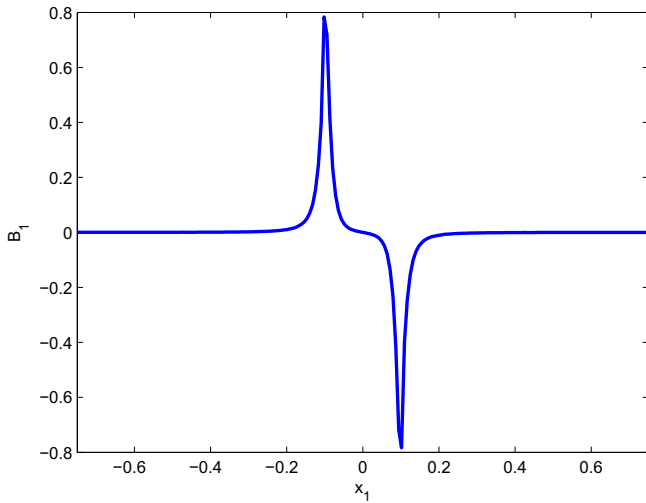


Fig. 3. Variation of B_1 along the horizontal line $x_2 = 0.01$. The maximum value of B_1 , close to the material interfaces, is about 0.8 Tesla. The component B_1 is normal to the material boundaries at $X_1 = \pm 0.1$ and is continuous across these interfaces.

rotation the point located at the intersection of edges (e) and (f) is not allowed to displace in the X_2 direction. The magnetic field component $H_2 = H$ on the boundaries (a) and (c) is given as $H = -10^6 \text{ Am}^{-1}$. In what follows the units of X_1 and X_2 are metres.

Fig. 3 illustrates the variation of the component B_1 of the magnetic induction vector along a horizontal line located at $x_2 = 0.01$ through the surrounding space and inside the material, and, in particular, its continuity at the interfaces. This shows that the magnitude of B_1 is essentially skew-symmetric along the X_1 direction, the slight difference being due to the lack of symmetry of the deformation with respect to the x_2 direction. The corresponding plot for $x_2 = -0.01$ (not shown) is essentially a reflection of that in Fig. 3 in the line $x_1 = 0$. The magnetic boundary condition requires that $B_1 = 0$ at $x_1 = \pm 2$. The magnitude of B_1 increases (decreases) rapidly as the material boundary is approached, reaches its maximum value at the interface, and within the material it returns to zero and switches sign. Note that $\mathbf{B} = \mu_0 \mathbf{H}$ in the surrounding space and that the unit of \mathbf{B} is Tesla $T = \text{NA}^{-1} \text{m}^{-1} = \text{kgA}^{-1} \text{s}^{-2}$ ($\mu_0 = 4\pi \cdot 10^{-7} \text{ NA}^{-2}$).

Fig. 4 shows the variation of the magnetic field component H_2 along a horizontal line located at $x_2 = 0.01$. On both sides of the material body, far away from the interfaces, the value of $H_2 = -10^6 \text{ Am}^{-1}$, equal to that applied to the far-field boundary,

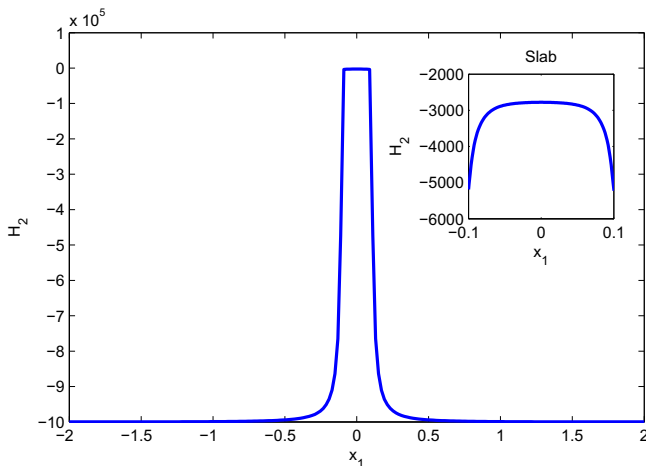


Fig. 4. Values of H_2 along the horizontal line $x_2 = 0.01$. Component H_2 is tangential to the left and right material interfaces and is continuous across these interfaces.

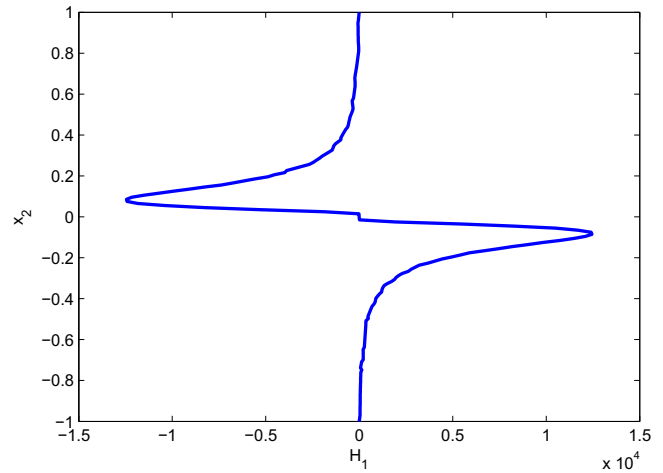


Fig. 5. Variation of H_1 with X_2 along the vertical line $x_1 = 0.01$. The component H_1 is tangential to the material boundaries located at $X_2 = \pm 0.02$ and is continuous across these interfaces.

i.e. the far field does not ‘feel’ the presence of the material body. As the material is approached the magnitude rapidly changes by several orders of magnitude. For clarity, the variation of H_2 inside the material is shown in the insert of the same figure.

Fig. 5 shows the changes of the component H_1 along a line defined by $x_1 = 0.01$. Recall that the undeformed configuration of the material is defined by the interval $-0.02 \leq X_2 \leq 0.02$ and that the component H_1 must be tangential to the material boundaries located at $X_2 = \pm 0.02$. This graph shows that outside the material, where the magnetic induction is connected to the magnetic field by $B_1 = \mu_0 H_1$, the field \mathbf{H} is essentially uniform and directed along the x_2 direction. Inside the material, in addition to \mathbf{B} and \mathbf{H} , we have the magnetization \mathbf{M} which, if needed, can be obtained using Eq. (3). As is the case with B_1 the distribution of H_1 is essentially skew-symmetric with respect to x_2 and also with respect to x_1 .

Figs. 6 and 7 show the deformed configuration of the material and contour plots of the spatial distributions of the magnitudes of the components B_1 and B_2 . The component B_1 is continuous across the left and right boundaries of the material and B_2 is continuous across the upper and lower boundaries. Obviously, due to the mechanical boundary conditions, the deformation is not symmetric with respect to x_2 . These contour plots also depict the deformed shape of the initially rectangular cross-section. In particular, the applied magnetic field induces a lateral contraction and axial elongation. The original straight boundaries do not remain straight and some outward bulging occurs.

An alternative representation of the magnetic induction \mathbf{B} is shown in Fig. 8. The magnetic field lines inside the material and in the surrounding space are represented by arrows with length proportional to the magnitude of \mathbf{B} . It shows that, due to symmetry and continuity requirements, the component B_1 essentially vanishes in the material and in the surrounding space except close to the edges (f) and (h). There is also a jump in the component B_2 across the same interfaces. Similarly, the jump conditions require that the component B_2 be continuous across the boundaries (e) and (g). The solid line indicates the boundary of the deformed body.

Contour plots of the components H_1 and H_2 , not shown separately, follow a very similar pattern to those for B_1 and B_2 inside the material body. Outside the body a contour plot of the magnitude of the magnetic field \mathbf{H} in the vicinity of the body is shown in Fig. 9, superimposed on the reference configuration. While the applied magnetic field is uniform with non-zero component in the x_2 direction away from the material, it becomes highly

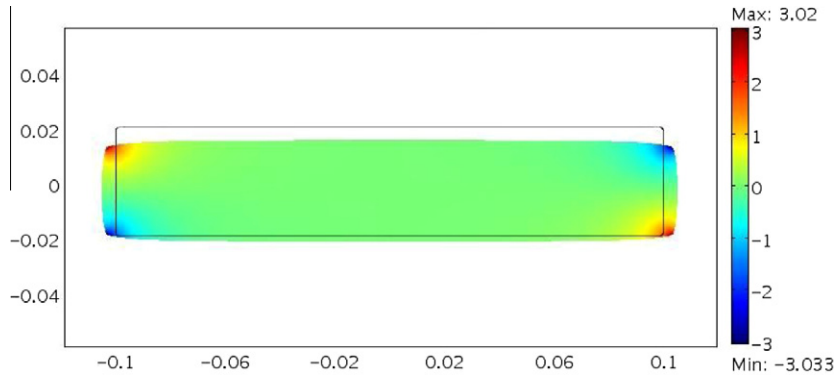


Fig. 6. Deformed configuration of the material body showing a lateral contraction and an axial extension of the material and a contour plot of B_1 , which is normal to the material interfaces located at $X_1 = \pm 0.1$, across which it is continuous.

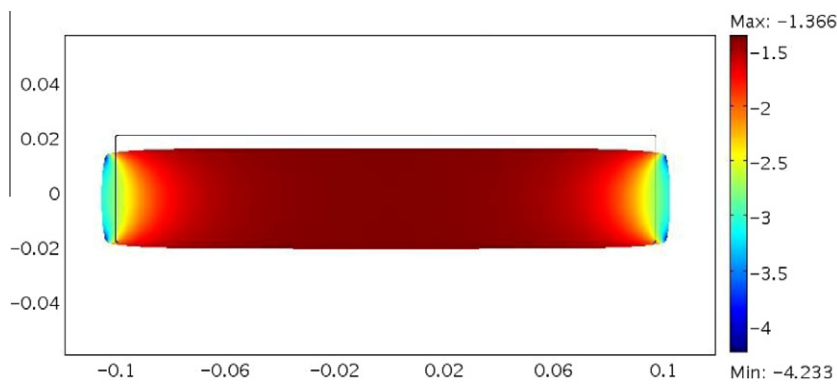


Fig. 7. Deformed configuration showing a lateral contraction and an axial extension of the material and a contour plot of B_2 , which is continuous across the material boundaries located at $X_2 = \pm 0.02$.

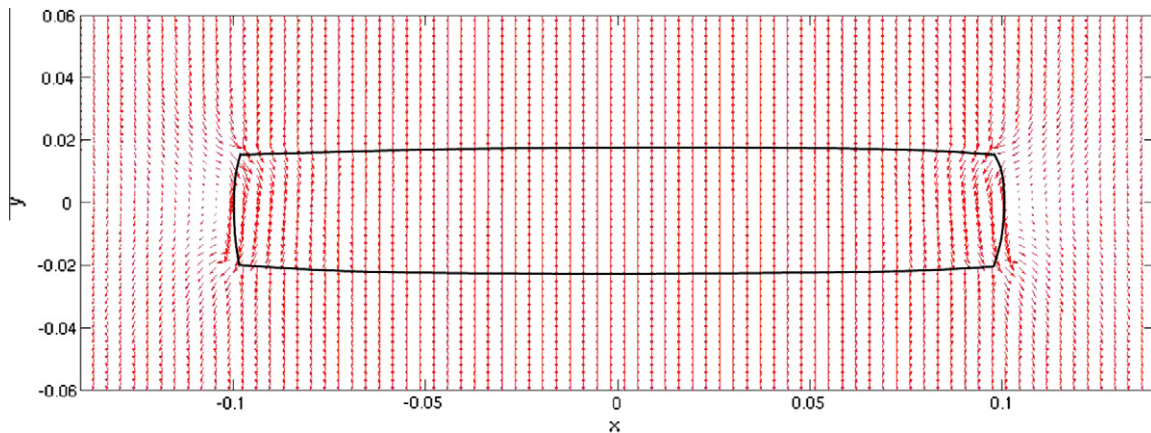


Fig. 8. Magnitude and direction of the field B inside the deformed material and in the surrounding space indicated by the arrows. The solid line shows the approximate deformed configuration of the magnetoelastic body.

non-uniform as the bounding surface of the magnetoelastic body is approached.

4.2. Example 2: shear deformation in a magnetic field

We again consider the geometry shown in Fig. 1 with boundary (e) now held fixed. Boundary (g) is not allowed to displace in the X_2 direction, but translates along the X_1 direction by the application of a uniform shear stress of 15 kPa. No mechanical loads are applied to the remaining boundaries (f) and (h). The magnetic field, in

the absence of the material body, is uniform and directed along the X_2 direction. It is defined as in Example 1, with $H_2 = H = -10^6 \text{ Am}^{-1}$.

Results in Fig. 10 show that the magnetic field, evaluated along a line located at $x_2 = 0.005$, remains uniform except in close proximity to the material boundaries at $X_1 = \pm 0.1$. The component H_2 is tangential to these boundaries and satisfies the continuity condition specified by (5)₂. The variation of the field component H_2 inside the material is shown by the insert to Fig. 10. Note that it is not symmetric with respect to x_1 .

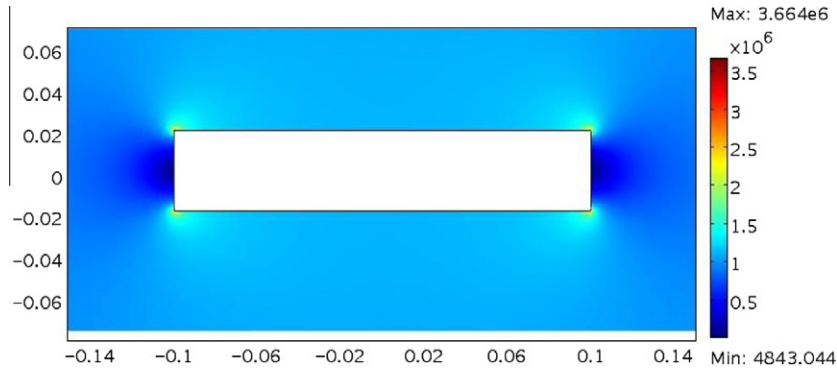


Fig. 9. Contour plot (based on the reference configuration) showing the magnitude of the magnetic field vector \mathbf{H} in the free space surrounding the material. The applied far-field magnetic field is uniform and has a magnitude of 10^6 Am^{-1} .

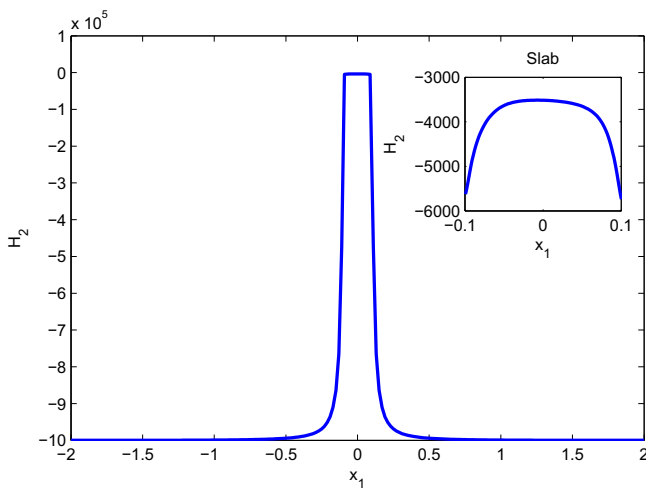


Fig. 10. Variation of H_2 along the line $x_2 = 0.005$, showing that the magnetic field is constant and uniform in most of the surrounding space, except in close proximity to the material boundaries $X_1 = \pm 0.1$. The insert shows the variation of H_2 inside the material.

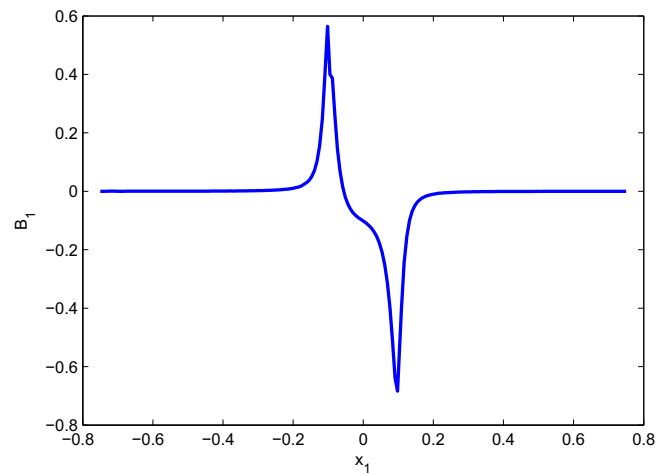


Fig. 11. Variation of B_1 inside the material body and in the surrounding space. The magnetic field is unidirectional in most of the free space except close to the material boundaries. Continuity conditions are satisfied at material interfaces $X_1 = \pm 0.1$. All values shown are determined along the line $x_2 = 0.005$.

The plot in Fig. 11 shows the variation of B_1 as a function of X_1 along a horizontal line located at $x_2 = 0.005$. In the surrounding space, due to the magnetic boundary conditions, the component B_1 vanishes everywhere except in close proximity to the material interfaces. At the material boundaries at $X_1 = \pm 0.1$, the absolute value reaches a maximum and satisfies the continuity conditions as specified by (5)₁. Note the non-symmetric character of the field in moving along the horizontal line $x_2 = 0.005$. Along the line $x_2 = 0.005$, the magnitude of the field is higher in the right half. Although not shown, along the horizontal line $x_2 = -0.005$, B_1 has a pattern that is close to a reflection of that for $x_2 = 0.005$ in the line $x_1 = 0$.

Variations of the component B_2 with respect to X_2 , evaluated along the lines defined by $x_1 = 0, 0.02, 0.05, 0.08$, are shown in Fig. 12. This component is normal to the material boundaries located at $X_2 = \pm 0.02$ and is continuous across them. The corresponding results along lines defined by $x_1 = -0.02, -0.05, -0.08$ (not shown) are identical, indicating that the component B_2 is symmetric with respect to the coordinate x_1 .

Fig. 13 shows the variation of the component H_1 in the free space and inside the material with X_2 along the line defined by $x_1 = 0.01$. This component is tangential to the boundaries at $X_2 = \pm 0.02$ and is continuous across these interfaces. The variation of the field component H_1 inside the material is shown by the small insert.

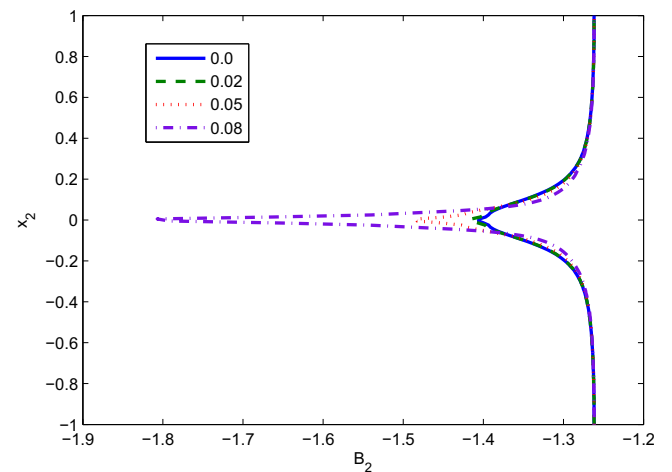


Fig. 12. Variation of B_2 with x_2 along the lines $x_1 = 0, 0.02, 0.05, 0.08$. The component B_2 is continuous across the material boundaries $X_2 = \pm 0.02$.

In Fig. 14 the deformed configuration of the material body is shown with the top boundary displaced parallel to the lower boundary, which is held fixed. The two lateral boundaries, denoted (h) and (f) in Fig. 1, are traction free and do not remain straight

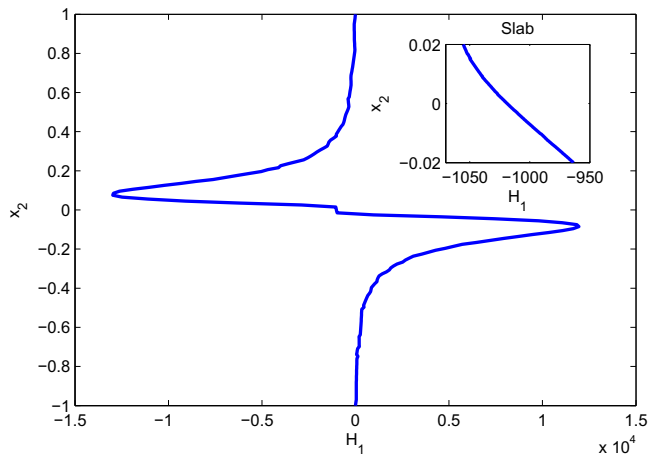


Fig. 13. Variation of H_1 along the line $x_1 = 0.01$, showing that the magnetic field is unidirectional in most of the free space, except close to the material boundaries. The component H_1 is tangent to the boundaries $x_2 = \pm 0.02$ and is continuous across these interfaces. The insert shows the variation of H_1 inside the material.

during the shear deformation. The deformation cannot therefore be described as *simple shear*. We refer to Dorfmann and Ogden (2005b) for a detailed discussion of a magnetoelastic body subject to simple shear deformation. The contour plot shows the magnitude of the total stress component τ_{12} inside the material body. There are high stresses in the lower left and upper right corner with magnitudes falling outside the selected range and therefore not captured by the colour coding.

5. Concluding remarks

In previous work (see, for example, Dorfmann and Ogden, 2005b) we have provided a limited number of exact solutions for boundary-value problems with infinite geometry where the magnetic boundary conditions can be satisfied exactly on all interfaces. However, such closed-form solutions are not in general possible when the geometry of the material body has finite dimensions. Thus, in order to find solutions to boundary-value problems it is necessary to adopt a numerical approach, and this paper has provided an illustration of this based on the finite element method, which appears not to have been used to any extent thus far for nonlinear magnetoelastic problems; see, however, the papers by Barham et al. (2009, 2010), which develop a finite element analysis of the deformation of thin magnetoelastic films. It should also be mentioned that for nonlinear *electroelastic* problems, a finite element formulation has been developed by Vu et al. (2007).

Here, we have examined two problems for a block of material with rectangular cross-section and infinite extent in the third direction subject to a uniform magnetic field applied far from the block and normal to the major faces of the block, the problem then being two-dimensional in character. In one problem no mechanical loads are applied and the deformation of the block is due entirely to the applied magnetic field, while in the second example the magnetic field is accompanied by shear tractions on its major faces (in the plane of the cross-section). Of particular concern was the satisfaction of the magnetic boundary conditions on the four faces of the block, which required determination of the magnetic field in the surrounding space as well as within the material.

For numerical purposes a simple prototype constitutive model of magnetoelasticity was adopted, and the results clearly show that for soft materials with high magneto-mechanical compliance large elastic deformations can be achieved under the influence of an external applied magnetic field, much larger than in conventional magnetostriction. Most importantly, however, the results show that the direction and magnitude of the magnetic field in the surrounding space, particularly in the vicinity of the material, are affected by the induced deformation, and these changes are reflected in the magnetic boundary conditions. Thus, it is important to consider the field within the surrounding space when the material body has finite geometry, especially where there are sharp changes in the geometry such as at a corner. Here, in order to avoid numerical problems we have taken the ‘corners’ to be slightly rounded. It would be of interest to investigate in future work if the rounding of the corners gives results that adequately approximate results for truly sharp corners.

The form of the energy function adopted will clearly have an influence on the results, but at present there are not enough relevant experimental data available to enable a truly experimentally based form of energy function to be constructed. We also note that the ALE formulation used for adjusting the exterior finite element mesh to follow the deformed shape of the boundary of the body does not provide a sufficiently accurate accommodation to the deforming boundary, and development of a more accurate method is therefore needed. Finally, we mention that for the values of the material constants used here the exterior Maxwell stress gave a negligible contribution to the traction of the boundary. For other values of the constants, for which the Maxwell stress was not negligible, it was difficult to obtain convergence of the solution. This, we believe, is partly because of the very rapid spatial variation in the magnetic field as the boundary is approached and partly because the Comsol implementation does not adapt the external mesh with sufficient accuracy to follow the *finitely* deforming boundary. For this reason we are currently developing our own finite element code to force the external mesh to follow the

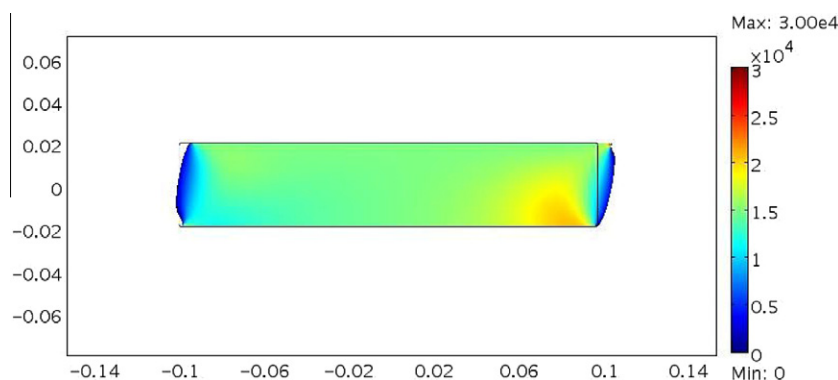


Fig. 14. The deformed configuration of the material and the associated contour plot of the shear component τ_{12} of the total stress tensor τ inside the material body.

deforming boundary more precisely in order to accommodate this deficiency.

Acknowledgements

Bustamante would like to express his gratitude for the financial support provided by FONDECYT (Chile) under Grant No. 11085024. Dorfmann acknowledges support from the United States – Israel Binational Science Foundation (BSF), Grant No. 2008419. The work of Ogden was supported by Grant No. EP/H016619/1 from the Engineering and Physical Sciences Research Council (UK), and by a grant from the Carnegie Trust for the Universities of Scotland.

References

- Albanese, A.M., Cunefare, K.A., 2003. Properties of magnetorheological semiactive vibration absorber. In: Agnes, G.S., Wang, K.-W. (Eds.), *Smart Structures and Materials: Damping and Isolation*, SPIE Proceedings, vol. 5052. SPIE Press, pp. 36–43.
- Barham, M.I., White, D.A., Steigmann, D.J., Rudd, R.E., 2009. Finite-element modeling of the deformation of a thin magnetoelastic film compared to a membrane model. *IEEE Trans. Magn.* 45, 4124–4127.
- Barham, M.I., White, D.A., Steigmann, D.J., 2010. Finite element modeling of the deformation of magnetoelastic film. *J. Comput. Phys.* 229, 6193–6207.
- Bednarek, S., 1999. The giant magnetostriction in ferromagnetic composites within an elastomer matrix. *Appl. Phys. A* 68, 63–67.
- Bellan, C., Bossis, G., 2002. Field dependence of viscoelastic properties of MR elastomers. *Int. J. Mod. Phys. B* 16, 2447–2453.
- Boczkowska, A., Awietjan, S.F., 2009. Smart composites of urethane elastomers with carbonyl iron. *J. Mater. Sci.* 44, 4104–4111.
- Bossis, G., Abbo, C., Cutillas, S., Lácis, S., Métayer, C., 2001. Electroactive and electrostructured elastomers. *Int. J. Mod. Phys. B* 15, 564–573.
- Brigadnov, I.A., Dorfmann, A., 2003. Mathematical modeling of magneto-sensitive elastomers. *Int. J. Solids Struct.* 40, 4659–4674.
- Brown, W.F., 1966. *Magnetoelastic Interactions*. Springer, Berlin.
- Bustamante, R., 2010. Transversely isotropic nonlinear magneto-active elastomers. *Acta Mech.* 210, 183–214.
- Bustamante, R., Dorfmann, A., Ogden, R.W., 2007. A nonlinear magnetoelastic tube under extension and inflation in an axial magnetic field: numerical solution. *J. Eng. Math.* 59, 139–153.
- Bustamante, R., Dorfmann, A., Ogden, R.W., 2008. On variational formulations in nonlinear magnetoelastostatics. *Math. Mech. Solids* 13, 725–745.
- Comsol Multiphysics, Version 3.4, 2007. Comsol Inc. Palo Alto, CA.
- Dorfmann, A., Ogden, R.W., 2003. Magnetoelastic modelling of elastomers. *Eur. J. Mech. A–Solids* 22, 497–507.
- Dorfmann, A., Ogden, R.W., 2004a. Nonlinear magnetoelastic deformations of elastomers. *Acta Mech.* 167, 13–28.
- Dorfmann, A., Ogden, R.W., 2004b. Nonlinear magnetoelastic deformations. *Quart. J. Mech. Appl. Math.* 57, 599–622.
- Dorfmann, A., Ogden, R.W., 2005a. Magnetomechanical interactions in magneto-sensitive elastomers. In: Austrell, P.-E., Kari, L. (Eds.), *Proceedings of the Third European Conference on Constitutive Models for Rubber*, Stockholm, Balkema, Rotterdam, pp. 531–543.
- Dorfmann, A., Ogden, R.W., 2005b. Some problems in nonlinear magnetoelasticity. *Z. Angew. Math. Phys. (ZAMP)* 56, 718–745.
- Eringen, A.C., Maugin, G.A., 1990. *Electrodynamics of Continua I*. Springer, New York.
- Farshad, M., Le Roux, M., 2004. A new active noise abatement barrier system. *Polym. Test.* 23, 855–860.
- Flory, P.J., 1961. Thermodynamic relations for high elastic materials. *Trans. Farad. Soc.* 57, 829–838.
- Ginder, J.M., Nichols, M.E., Elie, L.D., Tardiff, J.L., 1999. Magnetorheological elastomers: properties and applications. In: Wuttig, M.R. (Ed.), *Smart Structures and Materials: Smart Materials Technologies*, SPIE Proceedings, vol. 3675. SPIE Press, pp. 131–138.
- Ginder, J.M., Nichols, M.E., Elie, L.D., Clark, S.M., 2000. Controllable stiffness components based on magnetorheological elastomers. In: Wereley, N.M. (Ed.), *Smart Structures and Materials: Smart Structures and Integrated Systems*, SPIE Proceedings, vol. 3985. SPIE Press, pp. 418–425.
- Ginder, J.M., Schlotter, W.F., Nichols, M.E., 2001. Magnetorheological elastomers in tunable vibration absorbers. In: Inman, D.J. (Ed.), *Smart Structures and Materials: Damping and Isolation*, SPIE Proceedings, vol. 4331. SPIE Press, pp. 103–110.
- Ginder, J.M., Clark, S.M., Schlotter, W.F., Nichols, M.E., 2002. Magnetostrictive phenomena in magnetorheological elastomers. *Int. J. Mod. Phys. B* 16, 2412–2418.
- Hutter, K., van de Ven, A.A.F., Ursescu, A., 2006. *Electromagnetic Field Matter Interactions in Thermoelastic Solids and Viscous Fluids*. Springer, Berlin.
- Jackson, J.D., 1999. *Classical Electrodynamics*, third ed. John Wiley, New York.
- Jolly, M.R., Carlson, J.D., Muñoz, B.C., 1996. A model of the behaviour of magnetorheological materials. *Smart Mater. Struct.* 5, 607–614.
- Kankanala, S.V., Triantafyllidis, N., 2004. On finitely strained magnetorheological elastomers. *J. Mech. Phys. Solids* 52, 2869–2908.
- Kovetz, A., 2000. *Electromagnetic Theory*. University Press, Oxford.
- Li, W., Zhang, X., 2008. Research and applications of MR elastomers. *Recent Patents Mech. Eng.* 1, 161–166.
- Lokander, M., Stenberg, B., 2003. Performance of isotropic magnetorheological rubber materials. *Polym. Test.* 22, 245–251.
- Maugin, G.A., 1988. *Continuum Mechanics of Electromagnetic Solids*. North Holland, Amsterdam.
- Ogden, R.W., 1976. Volume changes associated with the deformation of rubber-like solids. *J. Mech. Phys. Solids* 24, 323–338.
- Ogden, R.W., 1978. Nearly isochoric elastic deformations: application to rubberlike solids. *J. Mech. Phys. Solids* 26, 37–57.
- Ogden, R.W., 1997. *Non-linear Elastic Deformations*. Dover, New York.
- Ogden, R.W., 2001. Elements of the theory of finite elasticity. In: Fu, Y.B., Ogden, R.W. (Eds.), *Nonlinear Elasticity: Theory and Applications*, London Mathematical Society Lecture Notes, vol. 283. Springer, Cambridge, pp. 1–57.
- Ogden, R.W., Steigmann, D.J., in press. *Mechanics and Electrodynamics of Magneto- and Electro-Elastic Materials*. CISM Courses and Lectures Series, vol. 527. Springer, Wien.
- Spencer, A.J.M., 1971. Theory of invariants. In: Eringen, A.C. (Ed.), *Continuum Physics*, vol. 1. Academic Press, New York, pp. 239–353.
- Steigmann, D.J., 2004. Equilibrium theory for magnetic elastomers and magnetoelastic membranes. *Int. J. Nonlinear Mech.* 39, 1193–1216.
- Varga, Z., Filipcsei, G., Szilágyi, A., Zrínyi, M., 2005. Electric and magnetic field-structured smart composites. *Macromol. Symp.* 227, 123–133.
- Varga, Z., Filipcsei, G., Zrínyi, M., 2006. Magnetic field sensitive functional elastomers with timeable modulus. *Polymer* 47, 227–233.
- Vu, D.K., Steinmann, P., Possart, G., 2007. Numerical modelling of non-linear electroelasticity. *Int. J. Numer. Methods Eng.* 70, 685–704.
- Yalcintas, M., Dai, H., 2004. Vibration suppression capabilities of magnetorheological materials based adaptive structures. *Smart. Mater. Struct.* 13, 1–11.